

$B_s \rightarrow \gamma\gamma$ decay in the two Higgs doublet model with flavor changing neutral currents

T. M. Aliev ,

Physics Department, Girne American University
Girne , Mersin-10, Turkey

E. O. Iltan *

Physics Department, Middle East Technical University
Ankara, Turkey

Abstract

We calculate the leading logarithmic QCD corrections to the decay $B_s \rightarrow \gamma\gamma$ in the two Higgs doublet model with tree level flavor changing currents (model III) including O_7 type long distance effects. Further, we analyse the dependencies of the branching ratio $Br(B_s \rightarrow \gamma\gamma)$ and the ratio of CP-even and CP-odd amplitude squares, $R = |A^+|^2/|A^-|^2$, on the charged Higgs mass m_{H^\pm} and the selected model III parameters $\xi^{U,D}$ including the leading logarithmic QCD corrections. It is found that to look for charged Higgs effects, the measurement of the branching ratio $Br(B_s \rightarrow \gamma\gamma)$ is promising.

*E-mail address: eiltan@heraklit.physics.metu.edu.tr

1 Introduction

Rare B meson decays constitute one of the most important classes of decays since they are induced by flavor changing neutral currents (FCNC) at loop level in the Standard Model (SM). Therefore they allow us to test the flavor structure of the SM and provide a comprehensive information about the fundamental parameters, such as Cabbibo-Kobayashi-Maskawa (CKM) matrix elements, leptonic decay constants, CP ratio, etc. These decays are also sensitive to the new physics beyond the SM, such as two Higgs Doublet model (2HDM), Minimal Supersymmetric extension of the SM (MSSM) [1], etc.

Among the rare B meson decays, the exclusive $B_s \rightarrow \gamma\gamma$ decay has received considerable interest in view of the planned experiments at the upcoming KEK and SLAC-B factories and existing hadronic accelerators, which may measure the branching ratios (Br) as low as 10^{-8} . Since the $B_s \rightarrow \gamma\gamma$ decay has two photon system, it is possible to study the CP violating effects [2] and it can be easily detected in the experiments by putting a cut for the energy of final photons [3]. Further, this decay can give information about physics beyond the SM.

The $B_s \rightarrow \gamma\gamma$ decay has been studied in the framework of the SM (2HDM) [2],[4]-[5] ([6]) without QCD corrections. It is well-known, that the QCD corrections to the $b \rightarrow s\gamma$ decay are considerably large (see [7] - [10] and references therein). Therefore, one can naturally expect that the situation is the same for the inclusive $b \rightarrow s\gamma\gamma$ decay. Recently, the analysis with the addition of the leading logarithmic (LLog) QCD corrections in the SM [11]-[13], 2HDM [14] and MSSM [15] has been done and the strong sensitivity to QCD corrections was obtained.

The calculations shows that the Br of the decay $B_s \rightarrow \gamma\gamma$ is enhanced with the addition of the QCD corrections in the SM. The extension of the Higgs sector (model II in 2HDM) brings extra enhancement to the Br . However, the present theoretical results are at the order of ($\sim 10^{-6}$) [14] are far from the experimental upper limit [16]

$$Br(B_s \rightarrow \gamma\gamma) \leq 1.48 \cdot 10^{-4} . \quad (1)$$

In the present work, we study this decay in the framework of the two Higgs doublet model with three level flavor changing neutral currents (model III) including perturbative QCD corrections in the LLog approximation, by imposing a method based on heavy quark effective theory for the bound state of the B_s meson [11]. Further, we improve our calculations with the inclusion of long-distance effects through the transition $B_s \rightarrow \phi\gamma \rightarrow \gamma\gamma$, which we call O_7 -type, see [11] for details. In the analysis, we use the constraints coming from $\Delta F = 2$ ($F = K, D, B$) mixing, the ρ parameter, the ratio $R_b^{exp} = \Gamma(Z \rightarrow b\bar{b})/\Gamma(Z \rightarrow hadrons)$ ($= 0.2178 \pm 0.0011$)

and the CLEO measurement of the decay $B \rightarrow X_s \gamma$ [17], for the selected parameters of model III [18], and we get an extreme enhancement for the $Br(B_s \rightarrow \gamma\gamma)$. We also predict an upper limit for the model III parameter $\bar{\xi}_{bb}^D$ using the present experimental restriction for the Br of the decay $B_s \rightarrow \gamma\gamma$, eq. (1).

The paper is organized as follows: In section 2, we give the LLog QCD corrected amplitude for the exclusive decay $B_s \rightarrow \gamma\gamma$. We further calculate the CP-odd A^- and CP-even A^+ amplitudes in an approach based on heavy quark effective theory, taking the LLog QCD corrections into account. Section 3 is devoted to the analysis of the dependencies of the Br and the ratio $|A^+|^2/|A^-|^2$ on the parameters μ (scale parameter), the Yukawa couplings $\bar{\xi}_{bb}^D, \bar{\xi}_{tt}^U$ and our conclusions. In the appendix , we present the operator basis and the Wilson coefficients responsible for the inclusive $b \rightarrow s\gamma\gamma$ decay in the model III. We also discuss the contributions of the neutral Higgs bosons to the coefficient C_7 for the decay $b \rightarrow s\gamma$ and the restrictions to the free parameters $\bar{\xi}_{ij}^D$, where one of the indices i or j belong to the first or second generation.

2 Leading logarithmic improved short-distance contributions in the model III for the decay $B_s \rightarrow \gamma\gamma$

In this section we present the effective Hamiltonian to the exclusive $B_s \rightarrow \gamma\gamma$ decay amplitude in the 2HDM with tree level neutral currents (model III). We start with the brief explanation of the model under consideration. The Yukawa interaction in the general case is

$$\mathcal{L}_Y = \eta_{ij}^U \bar{Q}_{iL} \tilde{\phi}_1 U_{jR} + \eta_{ij}^D \bar{Q}_{iL} \phi_1 D_{jR} + \xi_{ij}^U \bar{Q}_{iL} \tilde{\phi}_2 U_{jR} + \xi_{ij}^D \bar{Q}_{iL} \phi_2 D_{jR} + h.c. , \quad (2)$$

where L and R denote chiral projections $L(R) = 1/2(1 \mp \gamma_5)$, ϕ_i for $i = 1, 2$, are the two scalar doublets, $\eta_{ij}^{U,D}$ and $\xi_{ij}^{U,D}$ are the matrices of the Yukawa couplings. The choice of ϕ_1 and ϕ_2

$$\phi_1 = \frac{1}{\sqrt{2}} \left[\begin{pmatrix} 0 \\ v + H^0 \end{pmatrix} + \begin{pmatrix} \sqrt{2}\chi^+ \\ i\chi^0 \end{pmatrix} \right] ; \phi_2 = \frac{1}{\sqrt{2}} \begin{pmatrix} \sqrt{2}H^+ \\ H_1 + iH_2 \end{pmatrix} , \quad (3)$$

with the vacuum expectation values,

$$\langle \phi_1 \rangle = \frac{1}{\sqrt{2}} \begin{pmatrix} 0 \\ v \end{pmatrix} ; \langle \phi_2 \rangle = 0 , \quad (4)$$

permits us to write the Flavor Changing (FC) part of the interaction as

$$\mathcal{L}_{Y,FC} = \xi_{ij}^U \bar{Q}_{iL} \tilde{\phi}_2 U_{jR} + \xi_{ij}^D \bar{Q}_{iL} \phi_2 D_{jR} + h.c. , \quad (5)$$

where the couplings $\xi^{U,D}$ for the FC charged interactions are

$$\begin{aligned} \xi_{ch}^U &= \xi_{neutral} V_{CKM} , \\ \xi_{ch}^D &= V_{CKM} \xi_{neutral} , \end{aligned} \quad (6)$$

and $\xi_{neutral}^{U,D}$ ¹ is defined by the expression

$$\xi_N^{U,D} = (V_L^{U,D})^{-1} \xi^{U,D} V_R^{U,D} . \quad (7)$$

Here, the charged couplings appear as a linear combinations of neutral couplings multiplied by V_{CKM} matrix elements.

Now, we would like to discuss the LLog QCD corrections to $b \rightarrow s\gamma\gamma$ decay amplitude in the model III. As it is well known, the effective Hamiltonian method, obtained by integrating out the heavy degrees of freedom, is a powerful one. In the present case, t quark, W^\pm , H^\pm , H_1 , and H_2 bosons are the heavy degrees of freedom. Here H^\pm denote charged, H_1 and H_2 denote neutral Higgs bosons. The LLog QCD corrections are done through matching the full theory with the effective low energy theory at the high scale $\mu = m_W$ and evaluating the Wilson coefficients from m_W down to the lower scale $\mu \sim O(m_b)$. Note that we choose the higher scale as $\mu = m_W$ since the evaluation from the scale $\mu = m_{H^\pm}$ to $\mu = m_W$ gives negligible contribution to the Wilson coefficients ($\sim 5\%$) since the charged Higgs boson is heavy due to the current theoretical restrictions based on the experimental measurement of $B \rightarrow X_s\gamma$ due to the CLEO collaboration [17], for example, $m_{H^\pm} \geq 340 \text{ GeV}$ [19], $m_{H^\pm} \geq 480 \text{ GeV}$ [14].

The effective Hamiltonian relevant for our process is

$$\mathcal{H}_{eff} = -4 \frac{G_F}{\sqrt{2}} V_{tb} V_{ts}^* \sum_i C_i(\mu) O_i(\mu) , \quad (8)$$

where the O_i are operators given in eqs. (23), (24) and the C_i are Wilson coefficients renormalized at the scale μ . The coefficients C_i are calculated perturbatively. The explicit forms of the full-set operators and the corresponding Wilson coefficients are presented in Appendix.

To obtain the decay amplitude for the $B_s \rightarrow \gamma\gamma$ decay, we need to sandwich the effective Hamiltonian between the B_s and two photon states, i.e. $\langle B_s | \mathcal{H}_{eff} | \gamma\gamma \rangle$. This matrix element can be written in terms of two Lorentz structures [5] - [6], [11]-[13]:

$$\mathcal{A}(B_s \rightarrow \gamma\gamma) = A^+ \mathcal{F}_{\mu\nu} \mathcal{F}^{\mu\nu} + i A^- \mathcal{F}_{\mu\nu} \tilde{\mathcal{F}}^{\mu\nu} , \quad (9)$$

where $\tilde{\mathcal{F}}_{\mu\nu} = \frac{1}{2} \epsilon_{\mu\nu\alpha\beta} \mathcal{F}^{\alpha\beta}$. Here, the two different operator sets (eqs. (23) and (24)) give contributions to the CP-even A^+ and CP-odd A^- parts. We denote the CP-even (CP-odd) amplitudes due to the first set as A_1^+ (A_1^-) and the second set as A_2^+ (A_2^-). In a HQET inspired approach these amplitudes are:

$$A_1^+ = \frac{\alpha_{em} G_F}{\sqrt{2} \pi} \frac{f_{B_s}}{m_{B_s}^2} \lambda_t \left(\frac{1}{3} \frac{m_{B_s}^4 (m_b^{eff} - m_s^{eff})}{\bar{\Lambda}_s (m_{B_s} - \bar{\Lambda}_s) (m_b^{eff} + m_s^{eff})} C_7^{eff}(\mu) \right)$$

¹In all next discussion we denote $\xi_{neutral}^{U,D}$ as $\xi_N^{U,D}$.

$$\begin{aligned}
& - \frac{4}{9} \frac{m_{B_s^2}}{m_b^{eff} + m_s^{eff}} [(-m_b J(m_b) + m_s J(m_s))D(\mu) - m_c J(m_c)E(\mu)] , \\
A_1^- & = - \frac{\alpha_{em} G_F}{\sqrt{2}\pi} f_{B_s} \lambda_t \left(\frac{1}{3} \frac{1}{m_{B_s} \bar{\Lambda}_s (m_{B_s} - \bar{\Lambda}_s)} g_- C_7^{eff}(\mu) - \sum_q Q_q^2 I(m_q) C_q(\mu) \right. \\
& \left. + \frac{1}{9(m_b^{eff} + m_s^{eff})} [(m_b \Delta(m_b) + m_s \Delta(m_s))D(\mu) + m_c \Delta(m_c)E(\mu)] \right) , \quad (10)
\end{aligned}$$

and

$$\begin{aligned}
A_2^+ & = - \frac{\alpha_{em} G_F}{\sqrt{2}\pi} \frac{f_{B_s}}{m_{B_s}^2} \lambda_t \left(\frac{1}{3} \frac{m_{B_s}^4 (m_b^{eff} - m_s^{eff})}{\bar{\Lambda}_s (m_{B_s} - \bar{\Lambda}_s) (m_b^{eff} + m_s^{eff})} C_7^{teff}(\mu) \right) , \\
A_2^- & = - \frac{\alpha_{em} G_F}{\sqrt{2}\pi} f_{B_s} \lambda_t \left(\frac{1}{3} \frac{1}{m_{B_s} \bar{\Lambda}_s (m_{B_s} - \bar{\Lambda}_s)} g_- C_7^{teff}(\mu) \right) , \quad (11)
\end{aligned}$$

where $Q_q = \frac{2}{3}$ for $q = u, c$ and $Q_q = -\frac{1}{3}$ for $q = d, s, b$. Here, we have used the unitarity of the CKM-matrix $\sum_{i=u,c,t} V_{is}^* V_{ib} = 0$ and have neglected the contribution due to $V_{us}^* V_{ub} \ll V_{ts}^* V_{tb} \equiv \lambda_t$. The function g_- is defined as [11]:

$$g_- = m_{B_s} (m_b^{eff} + m_s^{eff})^2 + \bar{\Lambda}_s (m_{B_s}^2 - (m_b^{eff} + m_s^{eff})^2) . \quad (12)$$

The parameter $\bar{\Lambda}_s$ enters eq. (10) and (11) through the bound state kinematics [11]. Now, we would like explain the approach we follow to be clear how to get the amplitudes (eqs. (10) and (11)). The momentum of the \bar{b} -quark inside the B_s meson can be written as $p = m_b v + k$, where k is the residual momentum and v is the 4-velocity defined by $v = p_B / m_{B_s}$. Here p_B is the 4-momentum of the meson B_s . In the matrix elements we need to evaluate $p \cdot k_i$ and $p' \cdot k_i$, $i = 1, 2$, where k_i, p' are the momenta of the outgoing photon and s -quark respectively. We average the residual momentum of the \bar{b} quark as [20]

$$\begin{aligned}
\langle k_\mu \rangle & = - \frac{1}{2m_b} (\lambda_1 + 3\lambda_2) v_\mu , \\
\langle k_\mu k_\nu \rangle & = \frac{\lambda_1}{3} (g_{\mu\nu} - v_\mu v_\nu) , \quad (13)
\end{aligned}$$

where λ_1, λ_2 are matrix elements from heavy quark expansion. $\lambda_2 (= 0.12 \text{ GeV})$ can be determined from the $B_{(s)}^* - B_{(s)}$ mass splitting.

Finally we have

$$\begin{aligned}
p \cdot k_i & = \frac{m_{B_s}}{2} (m_{B_s} - \bar{\Lambda}_s) , \\
p' \cdot k_i & = - \frac{m_{B_s}}{2} \bar{\Lambda}_s , \\
(m_b^{eff})^2 & = p^2 = m_b^2 - 3\lambda_2 , \\
(m_s^{eff})^2 & = p'^2 = (m_s^{eff})^2 - m_{B_s}^2 + 2m_{B_s} \bar{\Lambda}_s . \quad (14)
\end{aligned}$$

Here, we use the definitions $p_B = p - p'$, $p_B \cdot k_i = \frac{m_{B_s}^2}{2}$, $v \cdot k_i = \frac{m_{B_s}}{2}$ and the HQET relation [20]

$$m_{B_s} = m_b + \bar{\Lambda}_s - \frac{1}{2m_b}(\lambda_1 + 3\lambda_2) , \quad (15)$$

In eq. (14), m_b^{eff} and m_s^{eff} are the effective masses of the quarks in the B_s meson bound state [11] and the parameter $\bar{\Lambda}_s$ can be defined as $\bar{\Lambda}_s = \bar{\Lambda} + \Delta m$. $\bar{\Lambda}$ together with λ_1 can be extracted from data on semileptonic B^\pm, B_0 decays [21] and the measured mass difference $\Delta m = m_{B_s} - m_B = 90 \text{ MeV}$ [22]. Using eq. (15), we correlate the parameters $\bar{\Lambda}_s$ and m_b and $\bar{\Lambda}$ and λ_1 (Table (1)).

After this brief explanation of the HQET inspired approach we follow, we continue with the LLog QCD-corrected Wilson coefficients $C_{1...10}(\mu)$ [11] - [13] which enter the amplitudes in the combinations

$$\begin{aligned} C_u(\mu) &= C_d(\mu) = (C_3(\mu) - C_5(\mu))N_c + C_4(\mu) - C_6(\mu) , \\ C_c(\mu) &= (C_1(\mu) + C_3(\mu) - C_5(\mu))N_c + C_2(\mu) + C_4(\mu) - C_6(\mu) , \\ C_s(\mu) &= C_b(\mu) = (C_3(\mu) + C_4(\mu))(N_c + 1) - N_c C_5(\mu) - C_6(\mu) , \\ D(\mu) &= C_5(\mu) + C_6(\mu)N_c , \\ E(\mu) &= C_{10}(\mu) + C_9(\mu)N_c \end{aligned} \quad (16)$$

where N_c is the number of colours ($N_c = 3$ for QCD).

The effective coefficients $C_7^{eff}(\mu)$ and $C_7'^{eff}(\mu)$ are defined in the NDR scheme, which we use here, as [18]

$$\begin{aligned} C_7^{eff}(\mu) &= C_7^{2HDM}(\mu) + Q_d (C_5^{2HDM}(\mu) + N_c C_6^{2HDM}(\mu)) , \\ &+ Q_u \left(\frac{m_c}{m_b} C_{10}^{2HDM}(\mu) + N_c \frac{m_c}{m_b} C_9^{2HDM}(\mu) \right) , \\ C_7'^{eff}(\mu) &= C_7'^{2HDM}(\mu) + Q_d (C_5'^{2HDM}(\mu) + N_c C_6'^{2HDM}(\mu)) \\ &+ Q_u \left(\frac{m_c}{m_b} C_{10}'^{2HDM}(\mu) + N_c \frac{m_c}{m_b} C_9'^{2HDM}(\mu) \right) . \end{aligned} \quad (17)$$

The functions $I(m_q)$, $J(m_q)$ and $\Delta(m_q)$ come from the irreducible diagrams with an internal q type quark propagating and are defined as

$$\begin{aligned} I(m_q) &= 1 + \frac{m_q^2}{m_{B_s}^2} \Delta(m_q) , \\ J(m_q) &= 1 - \frac{m_{B_s}^2 - 4m_q^2}{4m_{B_s}^2} \Delta(m_q) , \\ \Delta(m_q) &= \left(\ln \left(\frac{m_{B_s} + \sqrt{m_{B_s}^2 - 4m_q^2}}{m_{B_s} - \sqrt{m_{B_s}^2 - 4m_q^2}} \right) - i\pi \right)^2 \quad \text{for } \frac{m_{B_s}^2}{4m_q^2} \geq 1, \end{aligned}$$

$$\Delta(m_q) = - \left(2 \arctan\left(\frac{\sqrt{4m_q^2 - m_{B_s}^2}}{m_{B_s}}\right) - \pi \right)^2 \text{ for } \frac{m_{B_s}^2}{4m_q^2} < 1. \quad (18)$$

Finally the CP-even A^- and CP-odd A^+ amplitudes can be written as

$$\begin{aligned} A^+ &= A_1^+ + A_2^+ , \\ A^- &= A_1^- + A_2^- , \end{aligned} \quad (19)$$

where the amplitudes A_1^\pm and A_2^\pm are given in eqs. (10) and (11) respectively.

In our numerical analysis we used the input values given in Table (1).

Parameter	Value
m_c	1.4 (GeV)
m_b	4.8 (GeV)
α_{em}^{-1}	129
λ_t	0.04
$\Gamma_{tot}(B_s)$	$4.09 \cdot 10^{-13}$ (GeV)
f_{B_s}	0.2 (GeV)
m_{B_s}	5.369 (GeV)
m_t	175 (GeV)
m_W	80.26 (GeV)
m_Z	91.19 (GeV)
$\Lambda_{QCD}^{(5)}$	0.214 (GeV)
$\alpha_s(m_Z)$	0.117
λ_2	0.12 (GeV ²)
λ_1	-0.29 (GeV ²)
$\bar{\Lambda}_s$	590 (MeV)
$\bar{\Lambda}$	500 (MeV)

Table 1: Values of the input parameters used in the numerical calculations unless otherwise specified.

3 Discussion

Before we present our numerical results, we would like to discuss briefly the free parameters of the model under consideration, i.e. model III. This model induces many free parameters, such as $\xi_{ij}^{U,D}$ where i,j are flavor indices. To obtain qualitative results, we should restrict them using the experimental measurements. The explicit expressions of $C_7^{h_0}$ and $C_7^{A_0}$ (eq. (26)) show that the the neutral Higgs bosons can give a large contribution to the coefficient C_7 which can be in contradiction with the CLEO data [17],

$$Br(B \rightarrow X_s \gamma) = (2.32 \pm 0.07 \pm 0.35) 10^{-4} . \quad (20)$$

Such potentially dangerous terms are removed with the assumption that the couplings $\bar{\xi}_{N,is}^D$ ($i = d, s, b$) and $\bar{\xi}_{N,db}^D$ are negligible to be able to reach the conditions $\bar{\xi}_{N,bb}^D \bar{\xi}_{N,is}^D \ll 1$ and $\bar{\xi}_{N,db}^D \bar{\xi}_{N,ds}^D \ll 1$. Further, we use the constraints [18] coming from the ratio $R_b^{exp} = \Gamma(Z \rightarrow b\bar{b})/\Gamma(Z \rightarrow hadrons)$, namely $\xi_{Nbb}^D > \frac{60m_b}{v}$, the restrictions due to the $\Delta F = 2$ mixing, the ρ parameter [23], and the measurement by CLEO collaboration. The analysis of the mentioned processes and the discussion given above, leads to choose $\bar{\xi}_{Ntc} \ll \bar{\xi}_{Ntt}^U, \bar{\xi}_{Nbb}^D$ and $\bar{\xi}_{Nib}^D \sim 0, \bar{\xi}_{Nij}^D \sim 0$, where the indices i, j denote d and s quarks .

After these preliminary remarks, let us start with our numerical analysis. In this section we study the dependencies of the Br and the ratio $R = |A^+|^2/|A^-|^2$ on the selected parameters of the model III ($\bar{\xi}_{Ntt}^U, \bar{\xi}_{Nbb}^D$ and m_{H^\pm}) and the QCD scale μ . In figs. 1 and 2 (3 and 4) we plot the Br of the decay $B_s \rightarrow \gamma\gamma$ with respect to the charged Higgs mass m_{H^\pm} for the fixed value of $\bar{\xi}_{N,bb}^D = 60 m_b$ ($\bar{\xi}_{N,bb}^D = 90 m_b$) at three different μ scales ($\mu = 2.5, 5, m_W$) GeV . Fig. 1 (3) represents the case where the ratio $|r_{tb}| = \left| \frac{\bar{\xi}_{N,tt}^U}{\bar{\xi}_{N,bb}^D} \right| \ll 1$ and shows that the Br obtained in the model III almost coincides with the one calculated in the SM. The suppression of the contribution coming from the charged Higgs boson can be seen from eqs. (28) and 10 with the choice $|r_{tb}| \ll 1$. However in fig. 2 (4), the Br is presented for the case $r_{tb} \gg 1$. It is seen that there is an extreme enhancement of the Br , especially for the small values of m_{H^\pm} . Note that this is similar to the result coming from the choice of $\tan\beta < 1$ in the model II [14]. In figs. 5 (6) we present $\bar{\xi}_{N,bb}^D$ dependence of the Br at the fixed value of $m_{H^\pm} = 500 GeV$ for $|r_{tb}| \ll 1$ ($r_{tb} \gg 1$). In the region $|r_{tb}| \ll 1$, the Br is nonsensitive to the coupling $\bar{\xi}_{N,bb}^D$ and almost coincides with the SM value, however for $r_{tb} \gg 1$, it increases with the increasing $\bar{\xi}_{N,bb}^D$. Note that the Br is sensitive to the scale μ . For $|r_{tb}| \ll 1$, it increases with decreasing μ (figs. 1, 3 and 5) similar to the model II [14]. For $r_{tb} \gg 1$, decreasing the scale μ causes the Br to decrease. (figs. 2, 4 and 6).

At this stage we would like to estimate the upper limit of $\bar{\xi}_{N,bb}^D$ for $r_{tb} \gg 1$ by using the present experimental result $Br(B_s \rightarrow \gamma\gamma) \leq 1.48 \cdot 10^{-4}$. By choosing the lower limit for the mass $m_{H^\pm} \sim 480 \text{ GeV}$ [14] at the scale $\mu = 2.5 \text{ GeV}$, we get $\bar{\xi}_{N,bb}^D < 90 m_b$. It is interesting to note that the increasing value of m_{H^\pm} makes the restriction region for $\bar{\xi}_{N,bb}^D$ smaller.

Since the two photon system can be in a CP-even and CP-odd state, $B_s \rightarrow \gamma\gamma$ decay allows us to study CP violating effects. In the rest frame of the B_s meson, the $CP = -1$ amplitude A^- is proportional to the perpendicular spin polarization $\vec{\epsilon}_1 \times \vec{\epsilon}_2$, and the $CP = 1$ amplitude A^+ is proportional to the parallel spin polarization $\vec{\epsilon}_1 \cdot \vec{\epsilon}_2$. The ratio R is informative to search for CP violating effects in $B_s \rightarrow \gamma\gamma$ decays and it has been studied before in the literature in the framework of the 2HDM without [6] and with [14] QCD corrections.

Now, we present the dependence of the ratio $R = |A^+|^2/|A^-|^2$ on the selected parameters of model III, displayed in a series of figures (7 - 11). In figs. 7 and 8 we plot the dependence of R on m_{H^\pm} for fixed $\bar{\xi}_{N,bb}^D = 60 m_b$ and three different μ scales, $(2.5, 5, m_W) \text{ GeV}$. The R ratio is almost nonsensitive to m_{H^\pm} for $|r_{tb}| \ll 1$ (fig. 7). However, it is enhanced with the increasing value of m_{H^\pm} ($m_{H^\pm} \leq 1000 \text{ GeV}$) for $r_{tb} \gg 1$ (fig. 8). Decreasing the scale μ weakens the dependence of the ratio R on m_{H^\pm} and the contribution of the charged Higgs bosons to the R ratio becomes small similar to the model II [14]. Further, it becomes less dependent to m_{H^\pm} with increasing $\bar{\xi}_{N,bb}^D$ (fig 8, 9).

Fig. 10 and 11 show the dependence of R on $\bar{\xi}_{N,bb}^D$ for fixed $m_{H^\pm} = 500 \text{ GeV}$. Like the previous case, R dependence to the coupling $\bar{\xi}_{N,bb}^D$ is extremely weak for $|r_{tb}| \ll 1$. (fig. 10). For $r_{tb} \gg 1$ the ratio R increases with decreasing $\bar{\xi}_{N,bb}^D$ (fig 11). Note that, this ratio can exceed one unlike the SM case. The same situation appears in model II also [14].

The ratio R is quite sensitive to QCD corrections and it is enhanced with decreasing scale μ for the SM and $|r_{tb}| \ll 1$ (figs. 7, 10). However, this ratio decreases for $r_{tb} \gg 1$ (figs. 8, 9, 11). We observe, that the smaller the value of m_{H^\pm} (the larger the value of $\bar{\xi}_{N,bb}^D$), the less dependent is the ratio on μ . This strong μ dependence makes the analysis of the model III parameters m_{H^\pm} and $\bar{\xi}_{N,bb}^{U,D}$ for the given experimental value of the ratio R to be difficult, especially for the case $|r_{tb}| \ll 1$. However, we believe, that the strong μ dependence will be reduced with the addition the of next to leading order (NLO) calculation. This requires a computation of finite parts of many two loop diagrams, and divergent part of three-loop diagrams. This lies beyond the scope of the present work and it has to be done to reduce the uncertainty coming from the scale μ . Fortunately, the choice of $\mu = m_b/2$ in the LLog approximation reproduces effectively the NLO result for the $b \rightarrow s\gamma$ decay and one can suggest that it may also work for the $b \rightarrow s\gamma\gamma$

decay. In any case, the analysis on the model III parameters will be more reliable after NLO calculations are done.

We complete this section by taking the O_7 type long distance effects (LD_{O_7}) for both the Br and the ratio R into account. The LD_{O_7} contribution to the CP-odd A^- and CP-even A^+ amplitudes has been calculated with the help of the Vector Meson Dominance model (VMD) [11] and it was shown, that the influence on the amplitudes was destructive. With the addition of the LD_{O_7} effects, the amplitudes entering the Br and R ratio are now given as

$$\begin{aligned} A^+ &= A_{SD}^+ + A_{LD_{O_7}}^+, \\ A^- &= A_{SD}^- + A_{LD_{O_7}}^-, \end{aligned} \quad (21)$$

where A_{SD}^\pm are the short distance amplitudes we took into account in the previous sections (eq.(19)). The LD_{O_7} amplitudes $A_{LD_{O_7}}^\pm$ are defined as [11]

$$\begin{aligned} A_{LD_{O_7}}^+ &= -\sqrt{2}\frac{\alpha_{em}G_F}{\pi}\bar{F}_1(0)f_\phi(0)\lambda_t\frac{m_b(m_{B_s}^2 - m_\phi^2)}{3m_\phi m_{B_s}^2}C_7^{eff}(\mu), \\ A_{LD_{O_7}}^- &= \sqrt{2}\frac{\alpha_{em}G_F}{\pi}\bar{F}_1(0)f_\phi(0)\lambda_t\frac{m_b}{3m_\phi}C_7^{eff}(\mu), \end{aligned} \quad (22)$$

where $f_\phi(0) = 0.18 \text{ GeV}$ is the decay constant of ϕ meson at zero momentum, $\bar{F}_1(0)$ is the extrapolated $B_s \rightarrow \phi$ form factor (for details see [11]). Note that we neglect the contribution of operator O_7' in eq.(22) since the coefficient $C_7'^{eff}(\mu)$ is negligible compared to the coefficient $C_7^{eff}(\mu)$ (see the discussion given in appendix).

In figs. (12 - 17) we present the m_{H^\pm} and $\bar{\xi}_{N,bb}^D$ dependencies of the Br and the ratio R with the addition of LD_{O_7} effects. Here we use $\bar{F}_1(0) = 0.16$ [11]. The Br decreases with the addition of LD_{O_7} effects, since the effect is destructive. The μ scale uncertainty of the Br is smaller compared to the case where LD effect is not included.

It can be shown, that the value of the ratio R also decreases with the addition of LD_{O_7} effects for the SM case. (figs. 15 - 17). However, while m_{H^\pm} is increasing or $\bar{\xi}_{N,bb}^D$ is decreasing, the effect of the LD_{O_7} contribution on the ratio R is increasing for $r_{tb} \gg 1$ (figs. 16, 17).

There are still non-perturbative effects which can come from the formation of $c\bar{c}$ bound states. However these states are far off-shell and do not give significant contribution to the decay rate [13]. For example the chain process $B_s \rightarrow \phi\psi \rightarrow \phi\gamma \rightarrow \gamma\gamma$ is estimated and it is found to be at most 1% of the branching ratio $Br(B_s \rightarrow \gamma\gamma)_{SD+LD_{O_7}}$ [24]

Besides the strong μ dependence there is another uncertainty coming from the choice of bound state parameters m_b^{eff} and $\bar{\Lambda}_s$. It follows that the larger m_b^{eff} (smaller $\bar{\Lambda}_s$), the larger Br and R ratio. Here the enhancement of the Br is caused by the $\frac{1}{\bar{\Lambda}_s}$ dependence in amplitudes.

In conclusion, we analyse the selected model III parameters ($\bar{\xi}_{N,bb}^D, \bar{\xi}_{N,tt}^U, m_{H^\pm}$) and QCD scale μ dependencies of the Br and R ratio for the decay $B_s \rightarrow \gamma\gamma$. We predicted the upper bound for $\bar{\xi}_{N,bb}^D, \bar{\xi}_{N,bb}^U \leq 90 m_b$ in the case of $r_{tb} \gg 1$, using the constraints for $\bar{\xi}_{N,bb}^D, \bar{\xi}_{N,tt}^U$ [18] and the experimental upper limit for the Br of the decay under consideration. We obtain that the strong enhancement of the Br is possible in the framework of the model III.

A Appendix

The operator basis and the Wilson coefficients for the decay $b \rightarrow s\gamma\gamma$ in the model III

The operator basis is the same as the one used for the $b \rightarrow s\gamma$ decay in the model III [18] and $SU(2)_L \times SU(2)_R \times U(1)$ extensions of the SM [25]:

$$\begin{aligned}
O_1 &= (\bar{s}_{L\alpha}\gamma_\mu c_{L\beta})(\bar{c}_{L\beta}\gamma^\mu b_{L\alpha}), \\
O_2 &= (\bar{s}_{L\alpha}\gamma_\mu c_{L\alpha})(\bar{c}_{L\beta}\gamma^\mu b_{L\beta}), \\
O_3 &= (\bar{s}_{L\alpha}\gamma_\mu b_{L\alpha}) \sum_{q=u,d,s,c,b} (\bar{q}_{L\beta}\gamma^\mu q_{L\beta}), \\
O_4 &= (\bar{s}_{L\alpha}\gamma_\mu b_{L\beta}) \sum_{q=u,d,s,c,b} (\bar{q}_{L\beta}\gamma^\mu q_{L\alpha}), \\
O_5 &= (\bar{s}_{L\alpha}\gamma_\mu b_{L\alpha}) \sum_{q=u,d,s,c,b} (\bar{q}_{R\beta}\gamma^\mu q_{R\beta}), \\
O_6 &= (\bar{s}_{L\alpha}\gamma_\mu b_{L\beta}) \sum_{q=u,d,s,c,b} (\bar{q}_{R\beta}\gamma^\mu q_{R\alpha}), \\
O_7 &= \frac{e}{16\pi^2} \bar{s}_\alpha \sigma_{\mu\nu} (m_b R + m_s L) b_\alpha \mathcal{F}^{\mu\nu}, \\
O_8 &= \frac{g}{16\pi^2} \bar{s}_\alpha T_{\alpha\beta}^a \sigma_{\mu\nu} (m_b R + m_s L) b_\beta \mathcal{G}^{a\mu\nu}, \\
O_9 &= (\bar{s}_{L\alpha}\gamma_\mu c_{L\beta})(\bar{c}_{R\beta}\gamma^\mu b_{R\alpha}), \\
O_{10} &= (\bar{s}_{L\alpha}\gamma_\mu c_{L\alpha})(\bar{c}_{R\beta}\gamma^\mu b_{R\beta}),
\end{aligned} \tag{23}$$

and the second operator set $O'_1 - O'_{10}$ which are flipped chirality partners of $O_1 - O_{10}$:

$$\begin{aligned}
O'_1 &= (\bar{s}_{R\alpha}\gamma_\mu c_{R\beta})(\bar{c}_{R\beta}\gamma^\mu b_{R\alpha}), \\
O'_2 &= (\bar{s}_{R\alpha}\gamma_\mu c_{R\alpha})(\bar{c}_{R\beta}\gamma^\mu b_{R\beta}), \\
O'_3 &= (\bar{s}_{R\alpha}\gamma_\mu b_{R\alpha}) \sum_{q=u,d,s,c,b} (\bar{q}_{R\beta}\gamma^\mu q_{R\beta}), \\
O'_4 &= (\bar{s}_{R\alpha}\gamma_\mu b_{R\beta}) \sum_{q=u,d,s,c,b} (\bar{q}_{R\beta}\gamma^\mu q_{R\alpha}), \\
O'_5 &= (\bar{s}_{R\alpha}\gamma_\mu b_{R\alpha}) \sum_{q=u,d,s,c,b} (\bar{q}_{L\beta}\gamma^\mu q_{L\beta}),
\end{aligned}$$

$$\begin{aligned}
O'_6 &= (\bar{s}_{R\alpha}\gamma_\mu b_{R\beta}) \sum_{q=u,d,s,c,b} (\bar{q}_{L\beta}\gamma^\mu q_{L\alpha}), \\
O'_7 &= \frac{e}{16\pi^2} \bar{s}_\alpha \sigma_{\mu\nu} (m_b L + m_s R) b_\alpha \mathcal{F}^{\mu\nu}, \\
O'_8 &= \frac{g}{16\pi^2} \bar{s}_\alpha T_{\alpha\beta}^a \sigma_{\mu\nu} (m_b L + m_s R) b_\beta \mathcal{G}^{a\mu\nu}, \\
O'_9 &= (\bar{s}_{R\alpha}\gamma_\mu c_{R\beta}) (\bar{c}_{L\beta}\gamma^\mu b_{L\alpha}), \\
O'_{10} &= (\bar{s}_{R\alpha}\gamma_\mu c_{R\alpha}) (\bar{c}_{L\beta}\gamma^\mu b_{L\beta}), \tag{24}
\end{aligned}$$

where α and β are $SU(3)$ colour indices and $\mathcal{F}^{\mu\nu}$ and $\mathcal{G}^{\mu\nu}$ are the field strength tensors of the electromagnetic and strong interactions, respectively.

In the calculations, we take only the charged Higgs contributions into account and neglect the effects of neutral Higgs bosons. At this stage we would like to give the reasons by using the restrictions to the effective Wilson coefficient C_7^{eff} coming from the CLEO data in the process $B \rightarrow K^* \gamma$. (see section 2 and [18] also)

The neutral bosons H_0 , H_1 and H_2 are defined in terms of the mass eigenstates \bar{H}_0 , h_0 and A_0 as

$$\begin{aligned}
H_0 &= (\bar{H}_0 \cos\alpha - h_0 \sin\alpha) + v, \\
H_1 &= (h_0 \cos\alpha + \bar{H}_0 \sin\alpha), \\
H_2 &= A_0, \tag{25}
\end{aligned}$$

where α is the mixing angle and v is proportional to the vacuum expectation value of the doublet ϕ_1 (eq. (4)). Here we assume that the masses of neutral Higgs bosons h_0 and A_0 are heavy compared to the b-quark mass. The neutral Higgs scalar h_0 and pseudoscalar A_0 give contribution only to C_7 for our process. With the choice of $\alpha = 0$, $C_7^{h_0}$ and $C_7^{A_0}$ can be calculated at m_W level as

$$\begin{aligned}
C_7^{h_0}(m_W) &= (V_{tb}V_{ts}^*)^{-1} \sum_{i=d,s,b} \bar{\xi}_{N,bi}^D \bar{\xi}_{N,is}^D \frac{Q_i}{8 m_i m_b}, \\
C_7^{A_0}(m_W) &= (V_{tb}V_{ts}^*)^{-1} \sum_{i=d,s,b} \bar{\xi}_{N,bi}^D \bar{\xi}_{N,is}^D \frac{Q_i}{8 m_i m_b}, \tag{26}
\end{aligned}$$

where m_i and Q_i are the masses and charges of the down quarks ($i = d, s, b$) respectively. Here we used the redefinition

$$\xi^{U,D} = \sqrt{\frac{4G_F}{\sqrt{2}}} \bar{\xi}^{U,D}. \tag{27}$$

Eq. (26) shows that neutral Higgs bosons can give a large contribution to C_7 , which does not respect the CLEO data [17]. Here, we make an assumption that the couplings $\bar{\xi}_{N,is}^D$ ($i = d, s, b$)

and $\bar{\xi}_{N,db}^D$ are negligible to be able to reach the conditions $\bar{\xi}_{N,bb}^D \bar{\xi}_{N,is}^D \ll 1$ and $\bar{\xi}_{N,db}^D \bar{\xi}_{N,ds}^D \ll 1$. These choices permit us to neglect the neutral Higgs effects.

Denoting the Wilson coefficients for the SM with $C_i^{SM}(m_W)$ and the additional charged Higgs contribution with $C_i^H(m_W)$, we have the initial values for the first set of operators (eq.(23)) ([18] and references within)

$$\begin{aligned}
C_{1,3,\dots,6,9,10}^{SM}(m_W) &= 0 , \\
C_2^{SM}(m_W) &= 1 , \\
C_7^{SM}(m_W) &= \frac{3x^3 - 2x^2}{4(x-1)^4} \ln x + \frac{-8x^3 - 5x^2 + 7x}{24(x-1)^3} , \\
C_8^{SM}(m_W) &= -\frac{3x^2}{4(x-1)^4} \ln x + \frac{-x^3 + 5x^2 + 2x}{8(x-1)^3} , \\
C_{1,\dots,6,9,10}^H(m_W) &= 0 , \\
C_7^H(m_W) &= \frac{1}{m_t^2} (\bar{\xi}_{N,tt}^U + \bar{\xi}_{N,tc}^U \frac{V_{cs}^*}{V_{ts}^*}) (\bar{\xi}_{N,tt}^U + \bar{\xi}_{N,tc}^U \frac{V_{cb}}{V_{tb}}) F_1(y) , \\
&+ \frac{1}{m_t m_b} (\bar{\xi}_{N,tt}^U + \bar{\xi}_{N,tc}^U \frac{V_{cs}^*}{V_{ts}^*}) (\bar{\xi}_{N,bb}^D + \bar{\xi}_{N,sb}^D \frac{V_{ts}}{V_{tb}}) F_2(y) , \\
C_8^H(m_W) &= \frac{1}{m_t^2} (\bar{\xi}_{N,tt}^U + \bar{\xi}_{N,tc}^U \frac{V_{cs}^*}{V_{ts}^*}) (\bar{\xi}_{N,tt}^U + \bar{\xi}_{N,tc}^U \frac{V_{cb}}{V_{tb}}) G_1(y) , \\
&+ \frac{1}{m_t m_b} (\bar{\xi}_{N,tt}^U + \bar{\xi}_{N,tc}^U \frac{V_{cs}^*}{V_{ts}^*}) (\bar{\xi}_{N,bb}^D + \bar{\xi}_{N,sb}^D \frac{V_{ts}}{V_{tb}}) G_2(y) , \tag{28}
\end{aligned}$$

and for the second set of operators eq. (24),

$$\begin{aligned}
C_{1,\dots,10}'^{SM}(m_W) &= 0 , \\
C_{1,\dots,6,9,10}'^H(m_W) &= 0 , \\
C_7'^H(m_W) &= \frac{1}{m_t^2} (\bar{\xi}_{N,bs}^D \frac{V_{tb}}{V_{ts}^*} + \bar{\xi}_{N,ss}^D) (\bar{\xi}_{N,bb}^D + \bar{\xi}_{N,sb}^D \frac{V_{ts}}{V_{tb}}) F_1(y) , \\
&+ \frac{1}{m_t m_b} (\bar{\xi}_{N,bs}^D \frac{V_{tb}}{V_{ts}^*} + \bar{\xi}_{N,ss}^D) (\bar{\xi}_{N,tt}^U + \bar{\xi}_{N,tc}^U \frac{V_{cb}}{V_{tb}}) F_2(y) , \\
C_8'^H(m_W) &= \frac{1}{m_t^2} (\bar{\xi}_{N,bs}^D \frac{V_{tb}}{V_{ts}^*} + \bar{\xi}_{N,ss}^D) (\bar{\xi}_{N,bb}^D + \bar{\xi}_{N,sb}^D \frac{V_{ts}}{V_{tb}}) G_1(y) , \\
&+ \frac{1}{m_t m_b} (\bar{\xi}_{N,bs}^D \frac{V_{tb}}{V_{ts}^*} + \bar{\xi}_{N,ss}^D) (\bar{\xi}_{N,tt}^U + \bar{\xi}_{N,tc}^U \frac{V_{cb}}{V_{tb}}) G_2(y) , \tag{29}
\end{aligned}$$

where $x = m_t^2/m_W^2$ and $y = m_t^2/m_{H^\pm}^2$. The functions $F_1(y)$, $F_2(y)$, $G_1(y)$ and $G_2(y)$ are given as

$$\begin{aligned}
F_1(y) &= \frac{y(7 - 5y - 8y^2)}{72(y-1)^3} + \frac{y^2(3y-2)}{12(y-1)^4} \ln y , \\
F_2(y) &= \frac{y(5y-3)}{12(y-1)^2} + \frac{y(-3y+2)}{6(y-1)^3} \ln y ,
\end{aligned}$$

$$\begin{aligned}
G_1(y) &= \frac{y(-y^2 + 5y + 2)}{24(y-1)^3} + \frac{-y^2}{4(y-1)^4} \ln y , \\
G_2(y) &= \frac{y(y-3)}{4(y-1)^2} + \frac{y}{2(y-1)^3} \ln y .
\end{aligned} \tag{30}$$

Note that we neglect the contributions of the internal u and c quarks compared to one due to the internal t quark.

For the initial values of the Wilson coefficients in the model III (eqs. (28) and (29)), we have

$$\begin{aligned}
C_{1,3,\dots,6,9,10}^{2HDM}(m_W) &= 0 , \\
C_2^{2HDM}(m_W) &= 1 , \\
C_7^{2HDM}(m_W) &= C_7^{SM}(m_W) + C_7^H(m_W) , \\
C_8^{2HDM}(m_W) &= C_8^{SM}(m_W) + C_8^H(m_W) , \\
C'_{1,2,3,\dots,6,9,10}{}^{2HDM}(m_W) &= 0 , \\
C'_7{}^{2HDM}(m_W) &= C'_7{}^{SM}(m_W) + C'_7{}^H(m_W) , \\
C'_8{}^{2HDM}(m_W) &= C'_8{}^{SM}(m_W) + C'_8{}^H(m_W) .
\end{aligned} \tag{31}$$

At this stage it is possible to obtain the result for model II, in the approximation $\frac{m_s}{m_b} \sim 0$ and $\frac{m_b^2}{m_t^2} \sim 0$, by making the following replacements in the Wilson coefficients:

$$\begin{aligned}
\bar{\xi}_{st}^{U*} \bar{\xi}_{tb}^U &= m_t^2 \frac{1}{\tan^2 \beta} , \\
\bar{\xi}_{st}^{U*} \bar{\xi}_{tb}^D &= -m_t m_b ,
\end{aligned} \tag{32}$$

and taking zero for the coefficients of the flipped operator set, i.e $C'_i \rightarrow 0$.

The evaluation of the Wilson coefficients are done by using the initial values C_i^{2HDM} ($C_i'^{2HDM}$) and their contributions at any lower scale can be calculated as in the SM case [18].

References

- [1] J. L. Hewett, in proc. of the 21st Annual SLAC Summer Institute, ed. L. De Porcel and C. Dunwoode, SLAC-PUB6521.
- [2] S. Herrlich and J. Kalinowski , Nucl. Phys. B **381** (1992) 501.
- [3] L. Reina, G. Ricciardi and A. Soni, Phys. Lett B **396** (1997) 231.
- [4] G.-L. Lin, J. Liu and Y.-P. Yao, Phys. Rev. Lett. **64** (1990) 1498;
G.-L. Lin, J. Liu and Y.-P. Yao, Phys. Rev. D **42** (1990) 2314.
- [5] H. Simma and D. Wyler, Nucl. Phys. B **344** (1990) 283.
- [6] T. M. Aliev and G. Turan, Phys. Rev. D **48** (1993) 1176.
- [7] B. Grinstein, R. Springer, and M. Wise, Nucl. Phys. B**339** (1990) 269; R. Grigjanis, P.J. O'Donnel, M. Sutherland and H. Navelet, Phys. Lett. B**213** (1988) 355; Phys. Lett. B**286** (1992) E, 413; G. Cella, G. Curci, G. Ricciardi and A. Viceré, Phys. Lett. B**325** (1994) 227, Nucl. Phys. B**431** (1994) 417; M. Misiak, Nucl. Phys B**393** (1993) 23, Erratum B**439** (1995) 461.
- [8] K. G. Chetyrkin, M. Misiak and M. Münz, Phys. Lett.B **400** (1997) 206; C. Greub, T. Hurth and D. Wyler, Phys. Lett.B **380** (1996) 385; Phys. Rev. D **54** (1996) 3350.
- [9] M. Ciuchini, E. Franco, G. Martinelli, L. Reina and L. Silvestrini, Phys. Lett. B**316** (1993) 127; Nucl. Phys. B**421** (1994) 41.
- [10] A. J. Buras, M. Misiak, M. Münz and S. Pokorski, Nucl. Phys. B**424** (1994) 374.
- [11] G. Hiller and E. Iltan, Phys. Lett. B**409** (1997) 425.
- [12] C. H. V. Chang, G. L. Lin and Y. P. Yao, Phys. Lett. B**415** (1997) 395.
- [13] L. Reina, G. Ricciardi and A. Soni, Phys. Rev. D**56** (1997) 5085.
- [14] T. M. Aliev, G. Hiller and E. O. Iltan, Nucl. Phys. B**515** (1998) 321.
- [15] S. Bertolini and J. Matias, Phys. Rev. D **57** (1998) 4197.
- [16] M. Acciarri et al. (L3 Collaboration), Phys. Lett. B **363** (1995) 127.

- [17] M. S. Alam et al., CLEO Collaboration, Phys. Rev. Lett. **74** (1995) 2885.
- [18] T. M. Aliev, and E. Iltan, hep-ph/9803272,
- [19] M. Ciuchini et al. , hep-ph/9710335,
- [20] A. Manohar and M. B. Wise, Phys. Rev. D **49** (1994) 1310.
- [21] M. Gremm, A. Kapustin, Z. Ligeti and M. B. Wise, Phys. Rev. Lett. **77** (1996) 2.
- [22] R. M. Barnett et al., Review of Particle Properties, Phys. Rev. D**54** (1996) 1.
- [23] D. Atwood, L. Reina and A. Soni, Phys. Rev. D**55** (1997) 3156.
- [24] G. Hiller and E. O. Iltan, Mod. Phys. Lett. A **12** (1997) 2837.
- [25] P. Cho and Misiak, Phys. Rev. D **49** (1994) 5894.

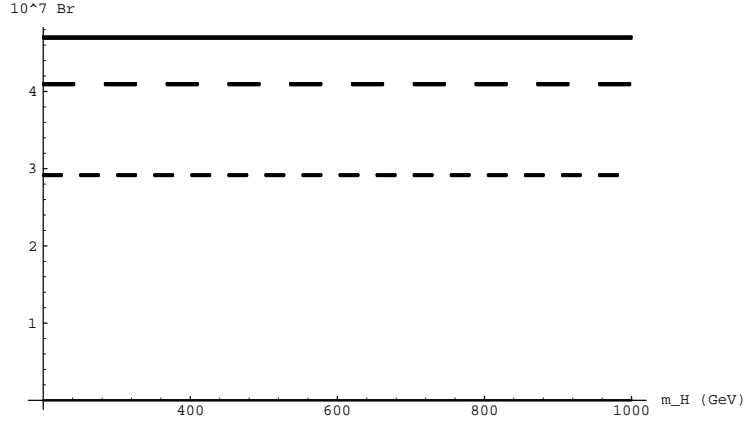


Figure 1: Br as a function of the mass m_{H^\pm} for fixed $\bar{\xi}_{N,bb}^D = 60 m_b$ at the region $|r_{tb}| \ll 1$. Here solid lines correspond to the scale $\mu = 2.5 \text{ GeV}$, dashed lines to $\mu = 5 \text{ GeV}$ and small dashed lines to $\mu = m_W \text{ GeV}$. The lines corresponding to the SM coincides with the lines we present here.

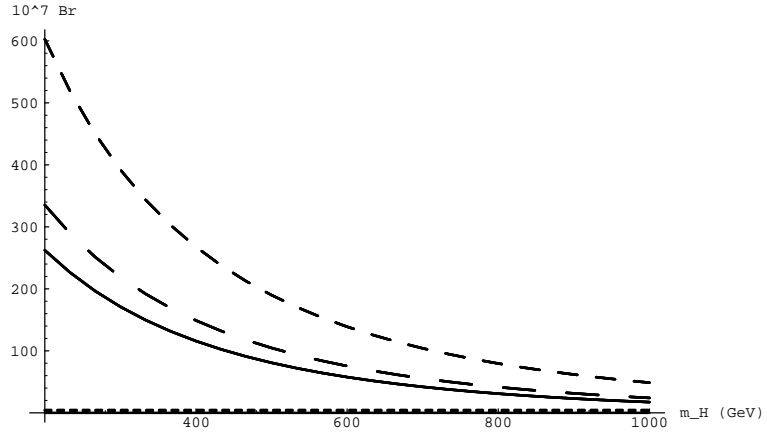


Figure 2: The same as Fig 1, but at the region $r_{tb} \gg 1$. Dotted dashed lines correspond to the SM. Note that dotted dashed line almost coincides with the m_H axis

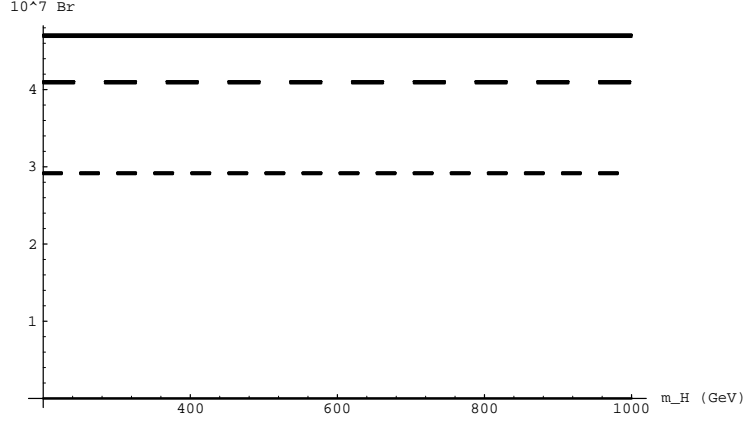


Figure 3: The same as Fig 1, but for fixed $\bar{\xi}_{N,bb}^D = 90 m_b$ value.

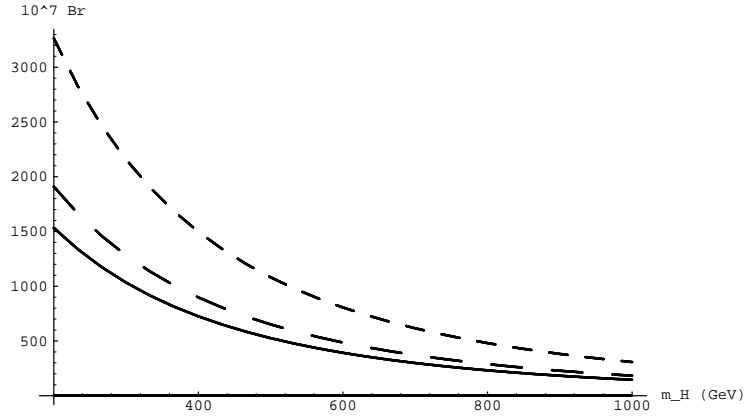


Figure 4: The same as Fig 2, but for fixed $\bar{\xi}_{N,bb}^D = 90 m_b$ value.

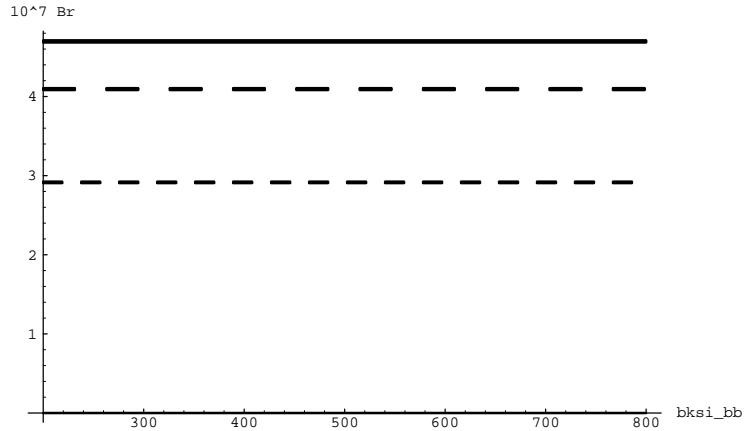


Figure 5: Br as a function of the coupling $\bar{\xi}_{N,bb}^D$ for fixed $m_{H^\pm} = 500 \text{ GeV}$ at the region $|r_{tb}| \ll 1$. Here solid lines correspond to the scale $\mu = 2.5 \text{ GeV}$, dashed lines to $\mu = 5 \text{ GeV}$ and small dashed lines to $\mu = m_W \text{ GeV}$. The lines corresponding to the SM coincides with the lines we present here.

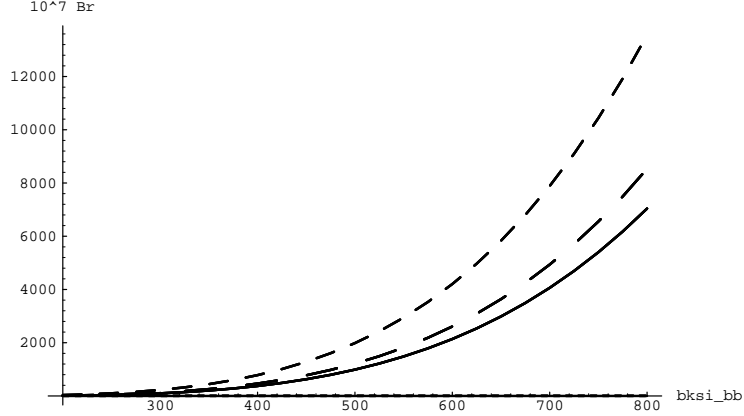


Figure 6: The same as Fig 5 but at the region $r_{tb} \gg 1$.

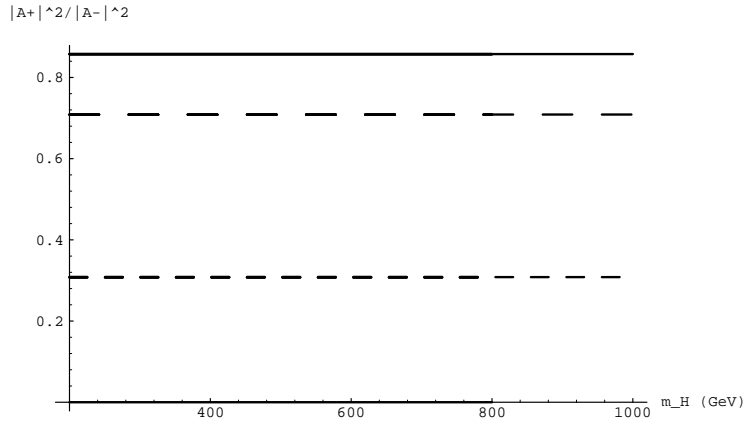


Figure 7: R ratio as a function of the mass m_{H^\pm} for fixed $\bar{\xi}_{N,bb}^D = 60 m_b$ at the region $|r_{tb}| \ll 1$. Here solid lines correspond to the scale $\mu = 2.5 \text{ GeV}$, dashed lines to $\mu = 5 \text{ GeV}$ and small dashed lines to $\mu = m_W \text{ GeV}$. The lines corresponding to the SM coincides with the lines we present here.

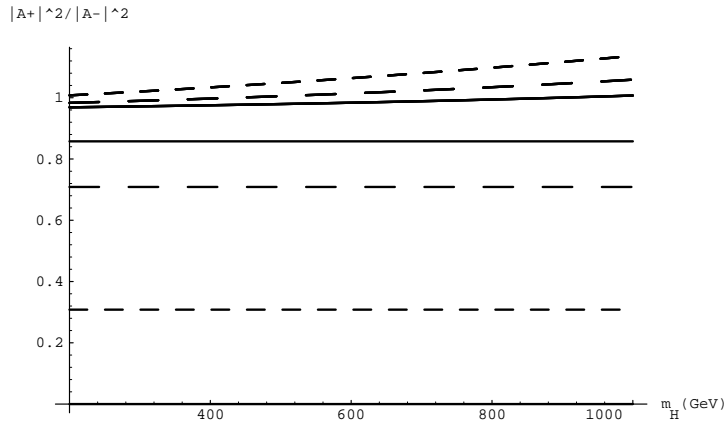


Figure 8: The same as Fig 7, but at the region $r_{tb} \gg 1$. Here solid curves (lines) correspond to the scale $\mu = 2.5 \text{ GeV}$, dashed curves (lines) to $\mu = 5 \text{ GeV}$ and small dashed curves (lines) to $\mu = m_W \text{ GeV}$ for model III (SM).

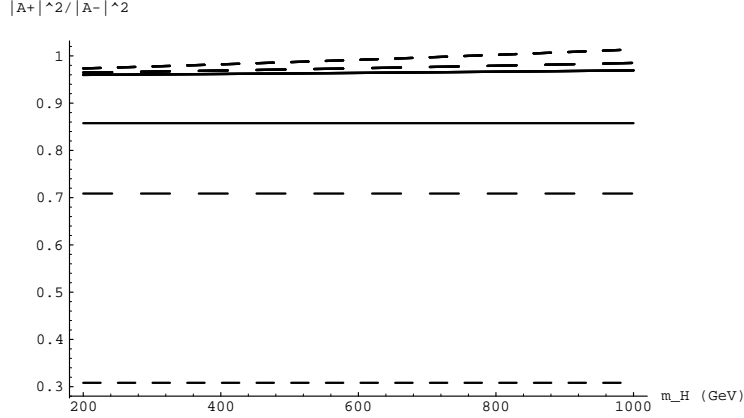


Figure 9: The same as Fig 8 but for fixed $\bar{\xi}_{N,bb}^D = 100 m_b$.

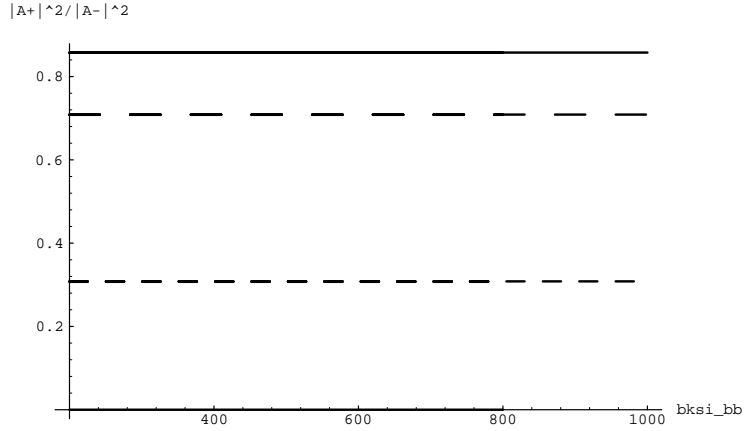


Figure 10: R ratio as a function of the coupling $\bar{\xi}_{N,bb}^D$ for fixed $m_{H^\pm} = 500 \text{ GeV}$ at the region $|r_{tb}| \ll 1$. Here solid lines correspond to the scale $\mu = 2.5 \text{ GeV}$, dashed lines to $\mu = 5 \text{ GeV}$ and small dashed lines to $\mu = m_W \text{ GeV}$. The lines corresponding to the SM coincides with the lines we present here.

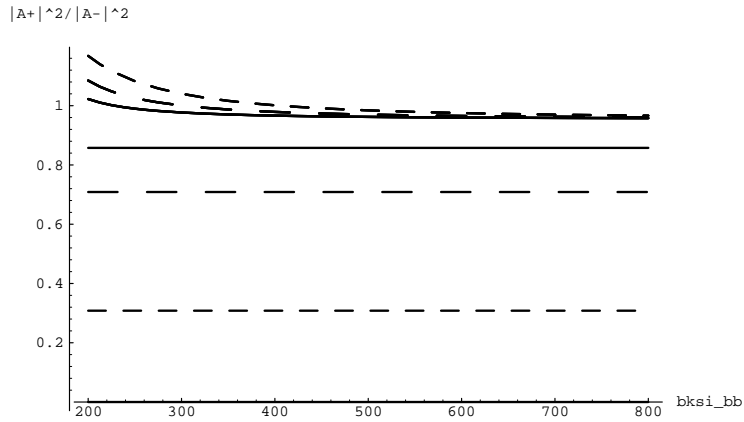


Figure 11: The same as Fig 7, but at the region $r_{tb} \gg 1$. Here solid curves (lines) correspond to the scale $\mu = 2.5 \text{ GeV}$, dashed lines to $\mu = 5 \text{ GeV}$ and small dashed lines to $\mu = m_W \text{ GeV}$ for model III (SM).

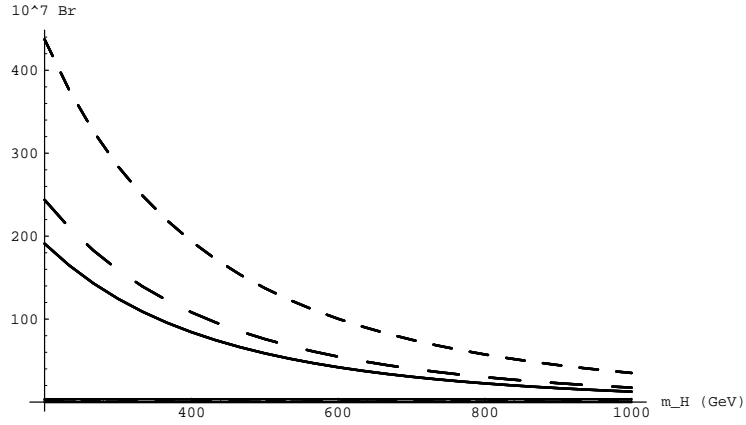


Figure 12: The same as Fig. 2 but including LD effects. The lines corresponding to the SM coincides almost with the m_{H^\pm} axis.

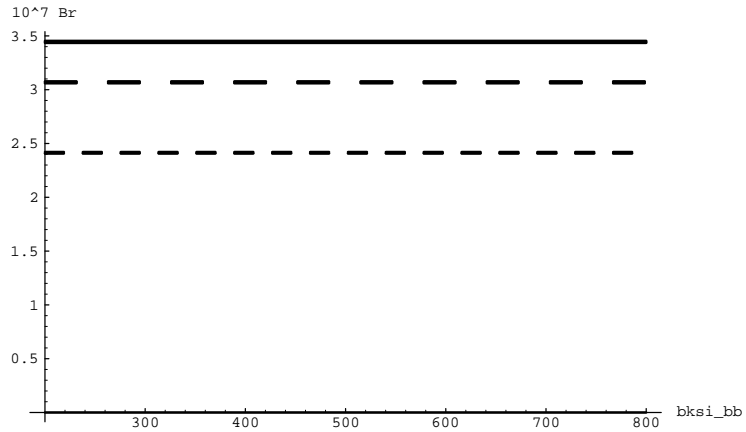


Figure 13: The same as Fig. 5 but including LD effects.

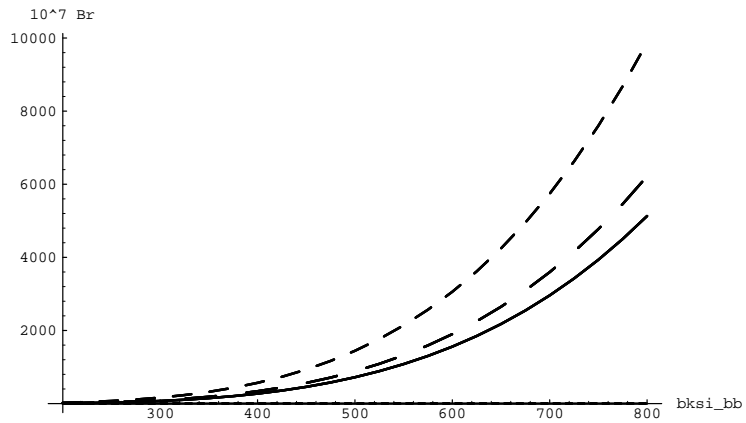


Figure 14: The same as Fig. 6 but including LD effects.

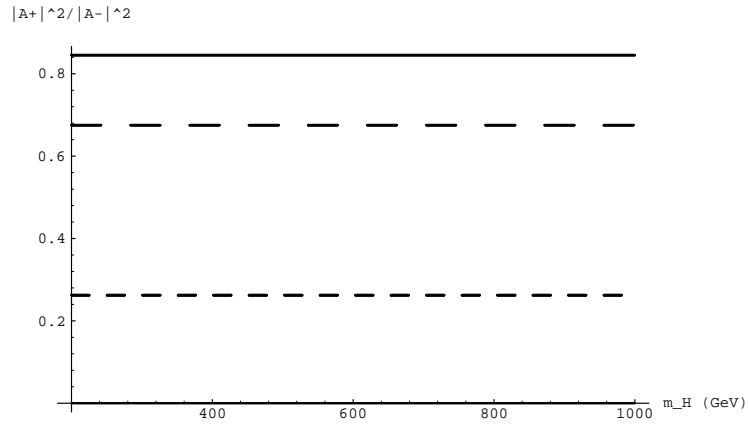


Figure 15: The same as Fig. 7 but including LD effects.

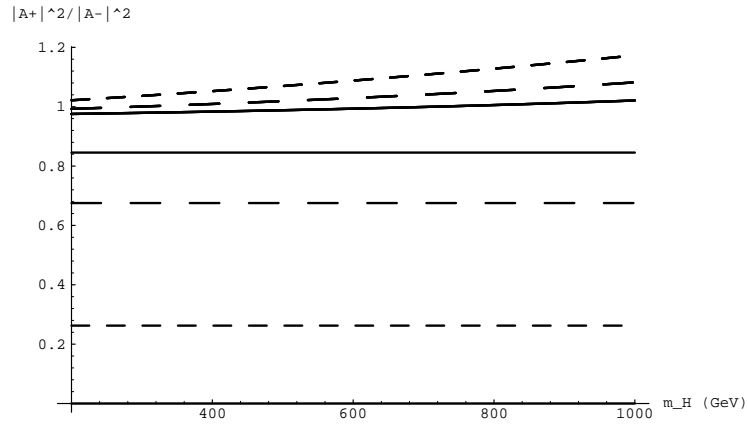


Figure 16: The same as Fig. 8 but including LD effects.

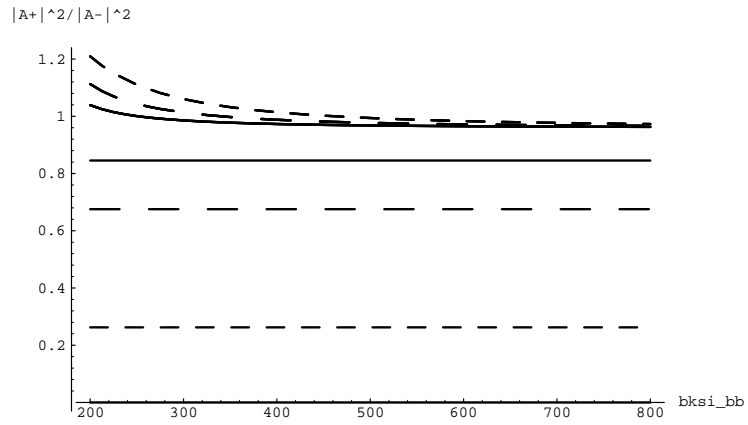


Figure 17: The same as Fig 11 , but including LD effects.